https://doi.org/10.5194/egusphere-2025-6533
Preprint. Discussion started: 12 February 2026

Resolving Systematic Errors in Sulfate Source Apportionment: A Field-Validated Kinetic Isotope Fractionation Framework

Zhaobing Guo[1,2], Xuexue Bai[1], Qiwei Ai[1], Zizheng Xu[1], Shangshun Ma[1], Jiayu Gu[3], Pengxiang Qiu[1], and Qingjun Guo[4]

[1]Jiangsu Key Laboratory of Atmospheric Environment Monitoring and Pollution Control (AEMPC), Collaborative Innovation Centre of Atmospheric Environment and Equipment Technology (CIC-AEET), School of Environmental Science and Engineering, Nanjing University of Information Science and Technology, Nanjing 210044, China
[2]Suqian University, Suqian 223800 China
[3]School of Chemical Engineering and Materials, Changzhou Institute of Technology, Changzhou 213032, China
[4]Center for Environmental Remediation, Institute of Geographic Sciences and Natural Resources Research, Chinese Academy of Sciences, Beijing 100101, China

Correspondence: Pengxiang Qiu (pxqiu@nuist.edu.cn) and Qingjun Guo (guoqj@igsnrr.ac.cn)

Abstract. Sulfates represent a critical constituent of atmospheric fine particulate matter ($PM_{2.5}$), significantly influencing air quality and climate dynamics. Precise quantification of atmospheric sulfate formation mechanisms and emission sources through stable isotope fractionation analysis represents a critical advancement in particulate matter pollution control. Conventional isotopic models relying on idealized complete SO_2 oxidation scenarios, while providing preliminary source apportionment estimates, exhibit systematic errors in reaction pathway quantification. Our field-validated approach incorporating actual atmospheric oxidation processes demonstrates that transition-metal ions (TMI)-catalyzed and NO_2-mediated pathways dominate sulfate production, with coal combustion (overestimate by 10.8% in summer) and traffic emissions (underestimated by 8.2% in summer) constituting primary sources. Comparative analysis reveals that traditional complete-oxidation models disproportionately diminish TMI pathway contributions, highlighting the necessity of kinetic fractionation corrections. These findings establish an improved isotopic tracing framework that resolves longstanding calculation discrepancies, delivering essential constraints for atmospheric sulfur cycle modeling and emission regulation strategies.

1 Introduction

Sulfate aerosols constitute a critical fraction of atmospheric particulate matter, with their formation mechanisms representing a pivotal yet unresolved aspect of air pollution control. The oxidation processes of sulfur dioxide (SO_2) exhibit remarkable mechanistic complexity stemming from its dual physicochemical nature(Kang et al., 2016). The exceptionally high hydration equilibrium constant drives near-instantaneous formation of S(IV) species (HSO_3^-/SO_3^{2-}), while the thermodynamically favorable oxidation potential creates a multidimensional reaction pathways including both homogeneous radical processes and heterogeneous interfacial reactions. These intrinsic reaction dynamics, when coupled with the extreme spatiotemporal variability of atmospheric conditions, create substantial obstacles for mechanistic elucidation under ambient environments. Current investigative approaches, including controlled laboratory simulations, field measurement, and computational modeling, each

https://doi.org/10.5194/egusphere-2025-6533
Preprint. Discussion started: 12 February 2026

face inherent limitations when applied in isolation. Laboratory studies inevitably simplify the unbounded nature of atmospheric systems, while field observations struggle to isolate specific chemical processes amid complex real-world interactions. Modeling studies, though valuable for hypothesis testing, remain constrained by incomplete mechanistic understanding and parameterization challenges. This methodological trilemma has resulted in persistent knowledge gaps regarding the dominant pathways and quantitative contributions of various sulfate formation mechanisms in different atmospheric regimes.

The application of stable isotope techniques in sulfate source attribution has emerged as a powerful analytical approach, leveraging the distinct isotopic fingerprints characteristic of different pollution sources and their remarkable stability during atmospheric transport.2 This methodology capitalizes on the system-specific fractionation patterns inherent to various sulfate formation pathways, which serve as critical tracers for reconstructing oxidation mechanisms. Contemporary research has quantitatively established the sulfur isotopic signatures (δ^{34}S)(Han et al., 2022; Yang et al., 2025) associated with major atmospheric oxidation routes, including transition metal ion-catalyzed (TMI, δ^{34}S= a), ozone-mediated (O_3, δ^{34}S = b), nitrogen oxide-driven (NO_x,δ^{34}S= c), and hydrogen peroxide-initiated (H_2O_2, δ^{34}S= d) pathways, through systematic analysis of particulate matter samples. Advanced mixing models, particularly Bayesian isotopic mixing approaches and Rayleigh fractionation formulations, have demonstrated considerable utility in deconvoluting sulfate sources and formation mechanisms. However, a fundamental limitation persists in current modeling frameworks that assume complete SO_2 oxidation (SOR = 1), an idealized condition rarely achieved in actual atmospheric chemistry. This oversimplification of sulfur transformation kinetics introduces systematic uncertainties in source apportionment, as the partial oxidation intermediates and kinetic isotope effects associated with incomplete SO_2 conversion are not adequately accounted for in conventional Rayleigh-based calculations.

Drawing conceptual inspiration from these insights, the present study pioneers a multi-model analytical framework that synergistically combines field observations with backward trajectory analysis Bayesian isotope mixing models and process-specific Rayleigh fractionation modeling. This integrated approach achieves precision in quantifying sulfate formation pathways while systematically addressing the critical but often neglected kinetic limitations inherent to incomplete SO_2 oxidation under real atmospheric conditions. By applying sulfur-oxygen isotope analysis to seasonally resolved aerosol samples from Nanjing, we demonstrate significant divergence between conventional complete-oxidation Rayleigh models and our kinetic fractionation-corrected framework. The systematic model intercomparison reveals substantial calibration requirements for stable isotope fractionation effects that have persistently biased previous sulfate source attribution studies. This methodological advancement establishes a new paradigm for urban sulfate pollution tracing particularly in complex emission environments where incomplete oxidation processes dominate. The seasonally differentiated results for Nanjing provide the observational evidence quantifying how traditional complete-oxidation assumptions distort source apportionment accuracy in both summer photochemical and winter coal-combustion dominated regimes.

https://doi.org/10.5194/egusphere-2025-6533
Preprint. Discussion started: 12 February 2026

2 Materials and methods

2.1 Sampling Sites

The atmospheric sampling protocol employed a monitoring site (118°43′E, 32°12′N) (Fig.S1) capturing seasonal extremes through January (winter) and July (summer) observations. A modified TH1000H high-volume sampler (Wuhan Tianhong Instrument) incorporated a dual-layer filtration assembly enabling concurrent $PM_{2.5}$ and SO_2 collection through co-laminated quartz (203×254 mm) and alkali-impregnated glass fiber filters (203×254 mm). Pre-treatment protocols involved muffle furnace combustion (450°C for 2h) followed by immersion in 2% K_2CO_3 + 2% glycerol solution for glass fiber filters. Sampling operations maintained 1.05 $m^3 \cdot min^{-1}$ flow rates during 24-hour cycles (08:00-08:00 local time) with meteorological parameters (wind speed/direction, temperature, pressure, humidity) continuously logged. Post-sampling handling included foil-wrapping (pre-combusted 450°C followed by 24-hour desiccation and dark refrigeration. The final dataset comprised samples after excluding precipitation events, with quartz filters positioned upstream for particulate collection and treated glass fiber membranes downstream for gaseous SO_2 capture.

2.2 Sample Collection

The ionic composition analysis of $PM_{2.5}$ samples was performed using Dionex ICS-3000 and ICS-2000 ion chromatography systems (Thermo Fisher Scientific) for simultaneous determination of major water-soluble ions. The analytical suite comprised five cations (Na^+, NH_4^+, K^+, Mg^{2+}, Ca^{2+}) and three anions (Cl^-, NO_3^-, SO_4^{2-}). The $\delta^{34}S$ value of sulfate was determined by precipitating $BaSO_4$ via $BaCl_2$ addition, followed by selective dissolution of residual $BaSO_3$ with 1 MHCl. After filtration and washing, the purified $BaSO_4$ was calcined at 1073 K for 2 h before analysis. Isotope ratios were measured using an elemental analyzer (EA, Flash 2000, Thermo) coupled to an isotope ratio mass spectrometer (IRMS, Delta V Plus, Finnigan).

Meteorological parameters and criteria air pollutant concentrations were acquired from two authoritative national databases during the sampling campaign. The China Meteorological Administration Data Service Center(http://data.cma.cn/) provided comprehensive weather records, while real-time air quality metrics were retrieved from the China National Environmental Monitoring Centre's online platform (www.aqistudy.cn/), representing the official monitoring network for atmospheric composition surveillance.

2.3 Trajectory Analysis Methodology

The source apportionment and transport pathways of $PM_{2.5}$ were investigated using the HYSPLIT 4.0 backward trajectory model developed by NOAA's Air Resources Laboratory (ARL). This analysis integrated the FNL meteorological database to reconstruct air mass movements. For each analysis period, trajectories were initialized at 500 m above ground level with a 72-hour temporal window. Four trajectories per day were computed at 6-hour intervals (00:00, 06:00, 12:00, and 18:00) to capture diurnal variations in atmospheric transport patterns.

https://doi.org/10.5194/egusphere-2025-6533
Preprint. Discussion started: 12 February 2026

2.4 Bayesian Stable Isotope Mixing Model

The source apportionment of sulfate aerosols was conducted through Stable Isotope Analysis in R (SIAR) modeling, a Bayesian framework that probabilistically quantifies contribution distributions and associated uncertainties from multiple emission sources by processing ambient $\delta^{34}S{-}SO_4^{2-}$ measurements(Parnell et al., 2010) alongside source-specific $\delta^{34}S$ signatures of precursor sulfur gases with all environmental samples maintaining consistent natural properties to eliminate cross-data variability particularly seasonal $\delta^{34}S{-}SO_4^{2-}$ fluctuations where the winter dataset (n=16) and summer dataset (n=15) were separately processed through SIAR to establish seasonally resolved sulfate source profiles for the Nanjing region.

The SIAR model determines the probability distribution of source contributions to mixtures and uncertainties associated with multiple sources(Fan et al., 2020a; Zheng et al., 2024; Harris et al., 2012a). In the SIAR framework, the isotopic value j in species i (X_{ij}) is expressed as:

$$X_{ij} = \frac{\sum_{k=1}^{k} p_k q_{jk}(S_{jk} + C_{jk})}{\sum_{k=1}^{k} p_k q_{jk}} + \varepsilon_{ij} \tag{1}$$

$$S_{jk} \backsim N(\mu_{jk}, \omega_{jk}^2) \tag{2}$$

$$\mathcal{C}_{jk} = (\lambda_{jk}, \tau_{jk}^2) \tag{3}$$

$$\varepsilon_{ij} \backsim (0, \sigma_j^2) \tag{4}$$

Where q_{jk} is isotopic value j in source; S_{jk} is source k for isotopej, normally distributed with mean (μ_{jk}) and variance (ω_{jk}^2); C_{jk} is isotopic enrichment factor for isotope j in source K, normally distributed with mean (λ_{jk}) and variance (τ_{jk}^2); (p_k) is proportion of source k; ε_{ij} is residual error representing unquantified variation between individual species, normally distributed with mean (0) and variance (σ_j^2).

2.5 Relative Contributions of SO_2 Oxidation Pathways to Sulfate Aerosols

Four sulfate formation pathways were considered: OH, H_2O_2/O_3, TMI, and NO_2 oxidation. Given the similar fractionation factors of H_2O_2 and O_3(Harris et al., 2012a, b; Lin et al., 2022), we used $\alpha_{H_2O_2/O_3}$ represent their combined fractionation. The temperature-independent $\alpha^{34}S$ fractionation factors are calculated as(Lin et al., 2022; Fan et al., 2020b):

$$\alpha^{34}S_{OH}(‰) = -(0.004 \pm 0.015) \times T + (10.60 \pm 0.73) \tag{5}$$

$$\alpha^{34}S_{H_2O_2/O_3}(‰) = -(0.085 \pm 0.004) \times T + (16.51 \pm 0.15) \tag{6}$$

https://doi.org/10.5194/egusphere-2025-6533
Preprint. Discussion started: 12 February 2026

$$\alpha^{34}S_{TMI}(‰) = -(0.237 \pm 0.004) \times T + (-5.039 \pm 0.044) \quad (7)$$

$$\alpha^{34}S_{NO_2}(‰) = exp[(0.2437 \pm 0.0457)/T + (0.0008 \pm 0.019)] \quad (8)$$

Where T is ambient temperature (°C). The total α^{34}S fractionation is computed as(Fan et al., 2020b; Sinha, 2013):

$$\alpha^{34}S = f_{OH} \times \alpha^{34}S_{OH} + f_{H_2O_2/O_3} \times \alpha^{34}S_{H_2O_2/O_3} + f_{TMI} \times \alpha^{34}S_{TMI} + f_{NO_2} \times \alpha^{34}S_{NO_2} \quad (9)$$

Where f_{OH},$f_{H_2O_2/O_3}$,f_{TMI} and f_{NO_2} , denote relative fractions of sulfate production from respective pathways, constrained by $\sum fx = 1$.

2.6 Sulfur Isotope Fractionation Modeling via Rayleigh Fractionation

Due to the absence of sulfur isotope equilibrium between atmospheric SO_2 and SO_4^{2-}, the Rayleigh Fractionation model can be applied to calculate the sulfur isotope fractionation effects between them. Within this framework, the δ^{34}S value of residual atmospheric SO_2 ($\delta^{34}S{-}SO_2$) is described by(Lin et al., 2022; Guo et al., 2019):

$$\alpha^{34}S - SO_2 = \delta^{34}S - SO_{2-emission} + \alpha^{34}S_{g\to p} \times ln(1 - SOR) \quad (10)$$

where $\alpha^{34}S_{g\to p}$ denotes the fractionation factor for SO_2(gaseous)$\longrightarrow SO_4^{2-}$(particles) conversion through gas and aqueous phases, $\delta^{34}S{-}SO_{2-emission}$ represents the δ^{34}S value of emission sources, and SOR is the SO_2 oxidation ratio, which can be calculated by the molar mass of SO_2 and SO_4^{2-}:

$$SOR = \frac{m(SO_4^{2-})/M(SO_4^{2-})}{m(SO_2)/M(SO_2) + m(SO_4^{2-})/M(SO_4^{2-})} \quad (11)$$

The source δ^{34}S value can be estimated from isotopic mass balance:

$$\delta^{34}S - SO_{2-emssion} = \delta^{34}S - SO_2 \times (1 - SOR) + \delta^{34}S - SO_4^{2-} \times SOR \quad (12)$$

where $\delta^{34}S{-}SO_4^{2-}$ is the observed δ^{34}S in sulfate. When SOR approaches 1 (complete SO_2 oxidation), $\delta^{34}S{-}SO_{2-emission}$ equals $\delta^{34}S{-}SO_4^{2-}$. The fractionation effects α is derived by combining Equations(10) and (12):

$$\alpha_{g\to p} = \frac{(\delta^{34}S - SO_{2-emssion} - \delta^{34}S - SO_4^{2-}) \times SOR}{(1 - SOR) \times ln(1 - SOR)} \quad (13)$$

To better understand this formula, we conducted α comparative analysis. The first scenario assumes Incomplete Oxidation Process of SO_2 (InCO Process) (SOR<1, partial conversion to SO_4^{2-}). The second scenario assumes Complete Oxidation Process of SO_2 (CO Process) (SOR=1, complete conversion to SO_4^{2-}).

https://doi.org/10.5194/egusphere-2025-6533
Preprint. Discussion started: 12 February 2026

3 Results and Discussion

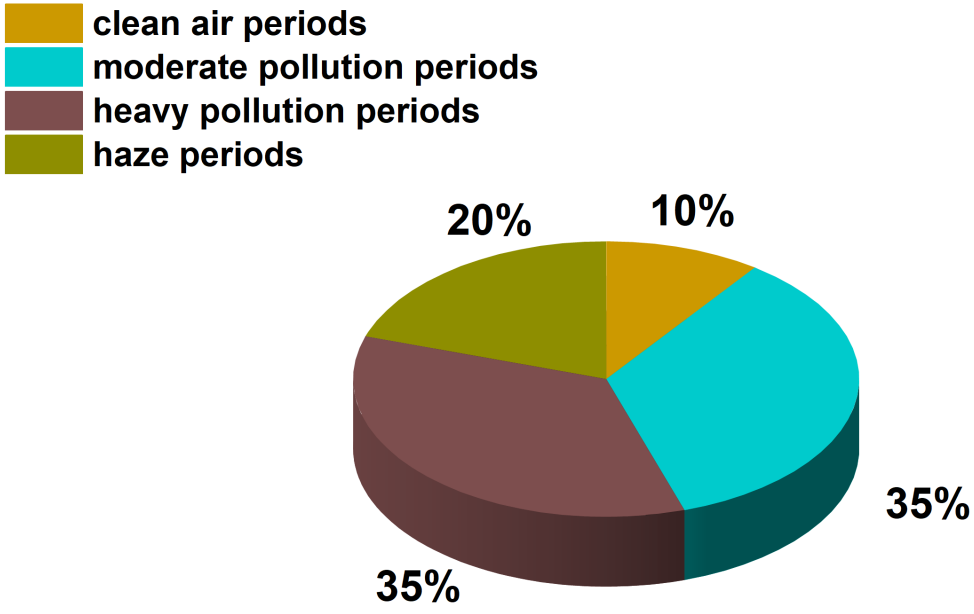

Figure 1. Proportion of different air mass periods

The chemical characterization of $PM_{2.5}$ in Nanjing identified sulfate (SO_4^{2-}) as the predominant water-soluble inorganic ion, comprising 27.9%-42.3% of the total ionic mass fraction, a finding that underscores persistent sulfate-driven aerosol pollution in the region. This pattern aligns with observations from other Chinese urban centers including Hangzhou (33.7%)(Lin et al., 2022), Guangzhou (40.2%-61.0%)(Tao et al., 2014b), and Beijing (33.0%)(Wei et al., 2018),collectively highlighting the prevalence of sulfate-rich $PM_{2.5}$ across China. Pollution episodes were categorized by $PM_{2.5}$ concentrations into clean ($\leq$35 μg m^{-3}), moderate (35-75 μg m^{-3}), heavy (75-150 μg m^{-3}), and haze (>150 μg m^{-3}) periods, with haze frequency (20%, Fig.1) doubling that of clean periods (10%). Sulfate concentrations exhibited pronounced pollution-dependence, peaking at 27.55$\pm$14.36 μg m^{-3}) during haze events 3.2 times higher than clean-phase levels (8.56$\pm$3.19 μg m^{-3}).

https://doi.org/10.5194/egusphere-2025-6533
Preprint. Discussion started: 12 February 2026

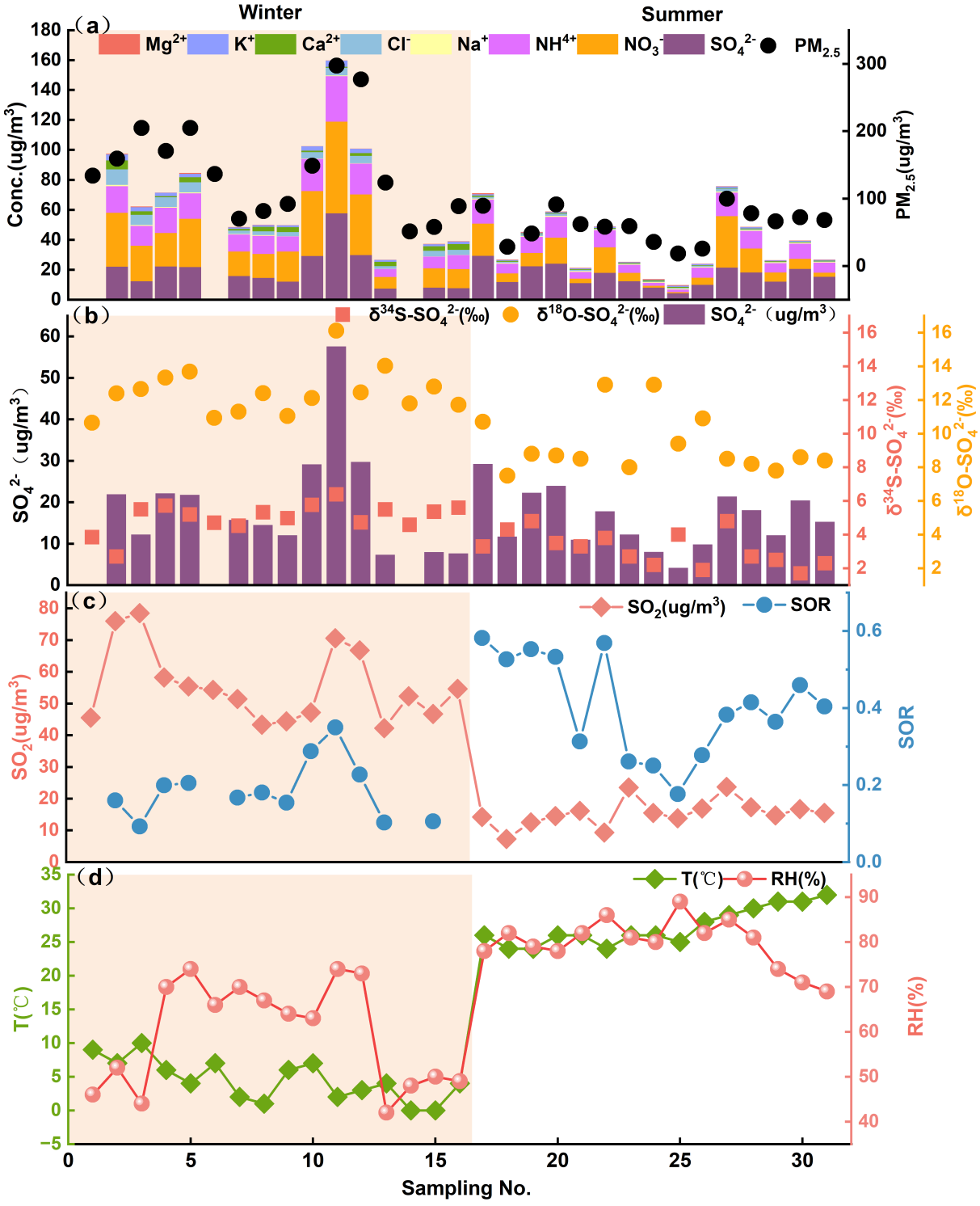

Figure 2. Time series of concentrations (values) of (a) $PM_{2.5}$ and ions, (b) $SO_4^{2}$and $\delta^{34}-SO_4^{2-}$,$\delta^{18}O-SO_4^{2-}$ (c) SO_2 and SOR, and (d) ambient temperature(T) and RH.

https://doi.org/10.5194/egusphere-2025-6533
Preprint. Discussion started: 12 February 2026

NH_4^+ and NO_3^- jointly accounted for 50.1%-57.9% of water-soluble ions (Fig.2a), while their strong covariation with SO_4^{2-} (Fig.2a,b) substantiates secondary sulfate formation as the principal $PM_{2.5}$ component and implicates combustion-derived emissions as its dominant source. The significant positive correlation between SO_4^{2-} and $PM_{2.5}$ concentrations (Fig.S3) further establishes sulfate's direct mechanistic role in particulate pollution escalation. The atmospheric source apportionment can be quantitatively assessed through the $[NO_3^-]/[SO_4^{2-}]$ mass ratio, where elevated values reflect increasing dominance of mobile versus stationary emission sources(Xiao et al., 2014; Arimoto et al., 1996).Our measurements yielded ratios spanning 0.15-1.95 (mean 0.98$\pm$0.42), exceeding Shanghai's 2002 baseline (0.43)(Yao et al., 2002) yet remaining below Jiaozuo's 2017 levels (1.36)(Zheng et al., 2024), collectively demonstrating Nanjing's intermediate position in mobile-source contribution among Chinese cities. These secondary aerosols originate through atmospheric oxidation of precursor gases, with SO_2 and NO_X principally derived from coal combustion and vehicular emissions respectively, while NH_3 predominantly stems from agricultural and livestock activities(Tao et al., 2014a). The strong inter-species correlations (Fig.S2a,S2b) confirm the co-formation of $(NH_4)_2SO_4$ and NH_4NO_3 through gas-to-particle conversion processes. The distinct sulfur and oxygen isotopic signatures (Fig.2b) observed across pollution periods unequivocally demonstrate temporal variations in sulfate formation pathways, necessitating mechanistic modeling to quantify the contribution ratios of specific reaction routes. Crucially, the persistent incomplete oxidation of sulfur dioxide to sulfate under all pollution conditions (Fig.2c) underscores the imperative for oxidation-process-constrained model optimization to elucidate the authentic atmospheric sulfate formation mechanisms.

https://doi.org/10.5194/egusphere-2025-6533
Preprint. Discussion started: 12 February 2026

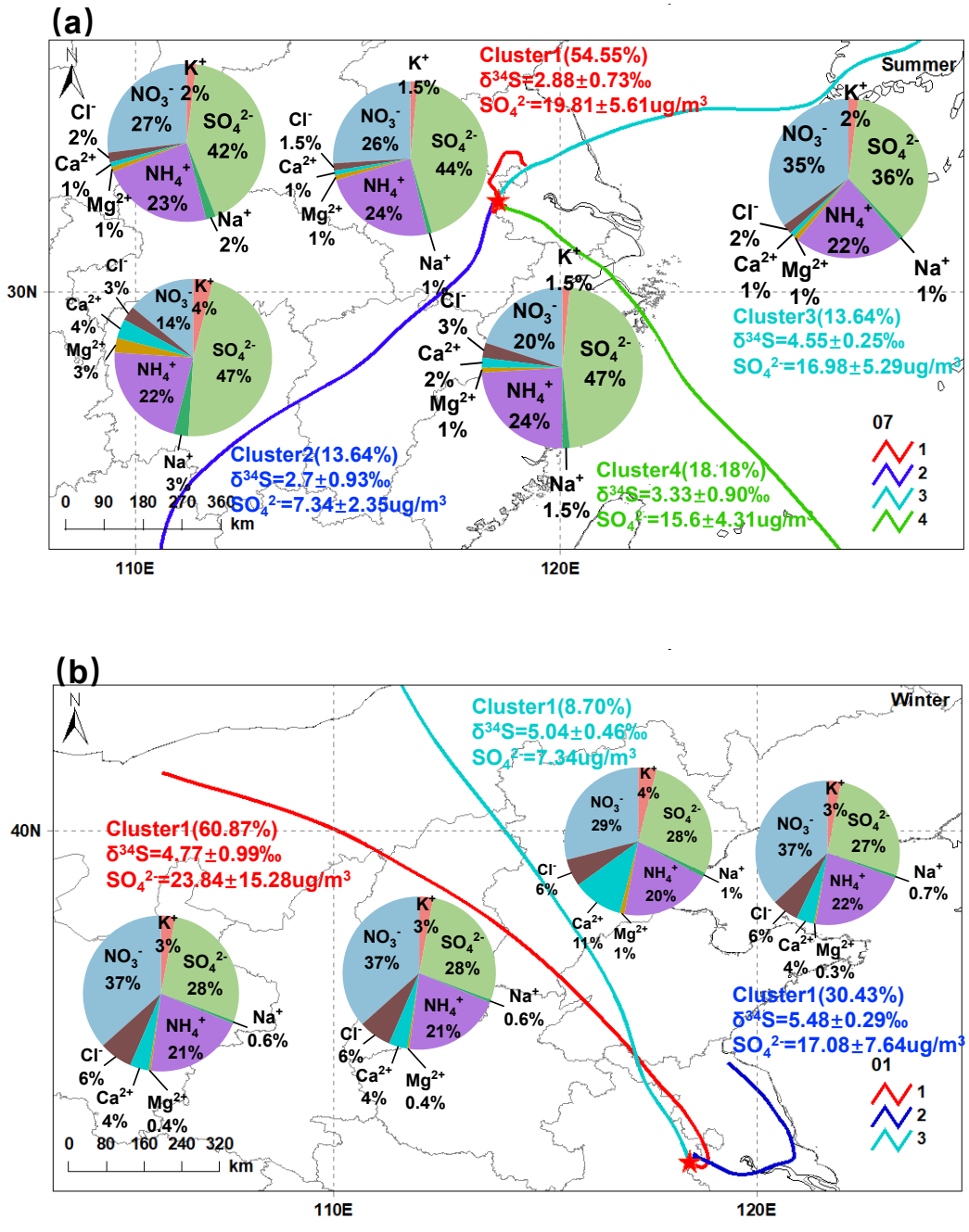

Figure 3. Pie charts of relative abundances of ions to TWSIIs and the $\delta^{34}S-SO_4^{2-}$ values in Nanjing for the different air clusters. The concentrations of TWSIIs and the $\delta^{34}S-SO_4^{2-}$ values are shown in the parentheses.(a:winter b:summer)}

https://doi.org/10.5194/egusphere-2025-6533
Preprint. Discussion started: 12 February 2026

The oxygen isotopic composition of atmospheric sulfate serves as a reliable indicator of oxidation pathways, with sulfate in $PM_{2.5}$ predominantly originating from SO_2 oxidation, consistent with established atmospheric chemistry. The $\delta^{34}S{-}SO_4^{2-}$ values (+1.7‰ to +6.3‰) of Nanjing sulfate aerosols, indicating coal combustion (+4.6‰ to +6.6‰) as the dominant source, thereby reflecting a greater coal-derived contribution relative to other Chinese regions. Cluster analysis of air mass trajectories reveals distinct seasonal patterns. During summer (Fig.3b), trajectories originating locally (54.55%), southwest China (13.64%), southeast China (18.18%), and the eastern Yellow Sea (13.64%) exhibit higher SO_4^{2-}concentrations locally (19.81 ± 5.61 μg m^{-3}) versus southwest (7.34 ± 2.35 μg m^{-3}), southeast (15.6 ± 4.31 μg m^{-3}), and Yellow Sea (16.98 ± 5.29 μg m^{-3}) sources, while $\delta^{34}S{-}SO_4^{2-}$ values show an inverse trend with lower values locally (2.88 ± 0.73‰) and in the southwest (2.70 ± 0.93‰) compared to southeast (3.33 ± 0.9‰) and Yellow Sea regions (4.55 ± 0.25‰), suggesting heterogeneous sources and formation mechanisms. Winter measurements (Fig.3a) display significant sulfate concentration disparities across back trajectories of air mass (e.g., Cluster 1: 23.84 ± 15.28 μg m^{-3}; Cluster 3: 7.34 μg m^{-3}) but statistically invariant $\delta^{34}S{-}SO_4^{2-}$ values (Cluster 1: 4.77 ± 0.99‰; Cluster 3: 5.04 ± 0.46‰); Northeastern Province(5.48 ± 0.29‰), with both concentration and $\delta^{34}S$ elevated versus summer, attributable to long-range transport of primary sulfates and coal-combustion emissions enriched in heavy isotopes. The significant negative correlation (Fig.2b,2d) between $\delta^{34}S$ and temperature arises as higher temperatures promote OH-mediated uniform oxidation, facilitating isotopic equilibrium fractionation during HSO_3^-/SO_4^{2-} exchange, which favors light-sulfur-isotope incorporation into sulfate and lowers summer $\delta^{34}S$(Han et al., 2016; Novák et al., 2001).Thus, secondary sulfate formation pathways and source variations primarily drive the observed winter-high/summer-low $\delta^{34}S$ pattern in $PM_{2.5}$, underscoring the mechanistic study's critical role in sulfate pollution control.

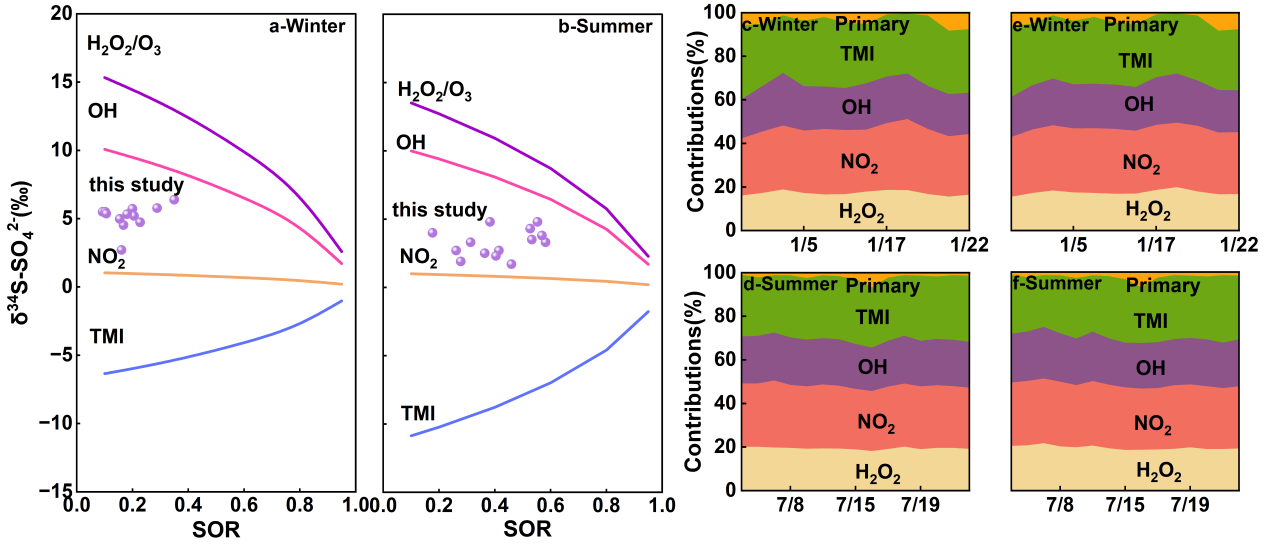

Figure 4. (ab) Rayleigh fractionation models for secondary SO_4^{2-}formation in different seasons. (cdef) Relative contributions of primary, OH, TMI,NO_2, and H_2O_2/O_3 pathways to secondary SO_4^{2-} generation across different seasons. (cd) represents the fractionation effects under InCO Process; (ef) represents the fractionation effects under CO Process.

https://doi.org/10.5194/egusphere-2025-6533
Preprint. Discussion started: 12 February 2026

The atmospheric sulfate formation pathways exhibit distinct sulfur isotope fractionation signatures, as demonstrated by theoretical calculations of $\delta^{34}S-SO_4^{2-}$ evolution under different oxidation mechanisms (Text.S2). Complete oxidation of SO_2 via H_2O_2/O_3 pathways would drive $\delta^{34}S-SO_4^{2-}$ depletion from 15.3‰ to 2.6‰ (Fig.4a), while OH-mediated oxidation would produce isotopic depletion from 11.8‰ to 3.4‰ (Fig.4a), both scenarios reflecting progressive sulfur oxidation (SOR 0 to 1). Conversely, exclusive $S(IV)+O_2(TMI)$ pathway participation would generate $\delta^{34}S-SO_4^{2-}$ enrichment from -6.4‰ to -1.0‰ (Fig.4a). These differential fractionation patterns confirm the coexistence of multiple sulfate production routes in the atmosphere, with all observed $\delta^{34}S-SO_4^{2-}$ values falling within the predicted theoretical ranges.

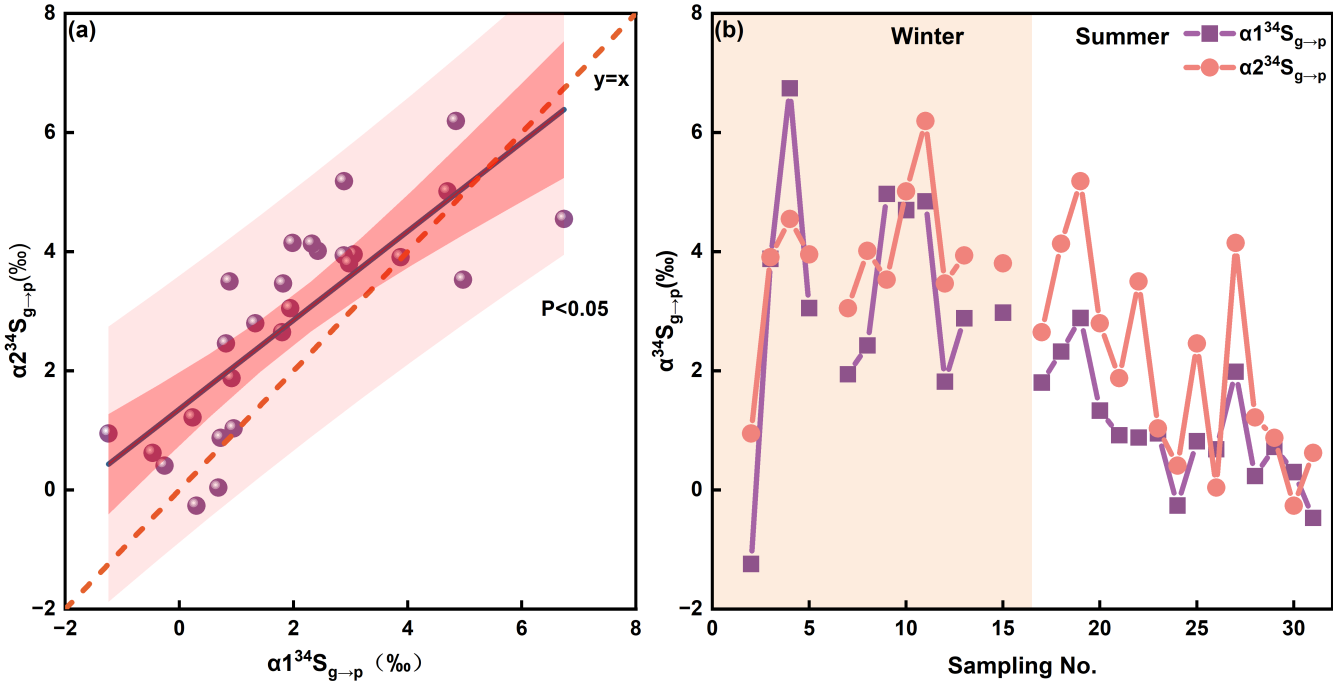

Figure 5. Linear regression between fractionation factor $\alpha 1$ (InCO Process) and fractionation factor $\alpha 2$ (CO Process). (The red line represents y = x [1:1 line], and the green line represents the fitted regression line between them.)

The isotopic fractionation factor α for sulfur isotopes was derived via Rayleigh fractionation models applied to $\delta^{34}S-SO_{2-emission}$ calculations based on atmospheric $\delta^{34}S-SO_4^{2-}$ and SOR, with synchronous field measurements (InCO Process) of $\delta^{34}S-SO_2$ averaging 1.7 ± 1.2‰ (range: -1.80 to +4.05‰) yielding α = 2.0± 1.8‰ (range: -1.2 to +6.7‰) (Fig.5b) per designated formula. Under complete oxidation (CO Process) (SOR=1), $\delta^{34}S-SO_4^{2-}$ demonstrated a significant negative correlation with SO ($\delta^{34}S-SO_4^{2-}$= -3.16SOR + 5.03; r = -0.36, p ≤ 0.05) (Fig.S4)), resulting in $\delta^{34}S-SO_{2-emission}$ of 1.8‰ at full conversion, which exceeds values from Shanghai (1.3‰)(Li et al., 2020), Hangzhou (1.5‰)(Lin et al., 2022), and Jiaozuo (1.7‰)(Zheng et al., 2024) and represents the pre-transformation source signature. An alternative α calculation (formula 9) generated a mean of 2.8 ± 1.7‰ (range: -0.2 to +6.1‰), higher than Guangzhou (<1.5‰)(Fan et al., 2020c) but lower than Beijing (4.2 ± 1.2‰)(Mang et al., 2018) with elevated α in central China attributable to temperature-dependent fractionation increases

https://doi.org/10.5194/egusphere-2025-6533
Preprint. Discussion started: 12 February 2026

(Fig.S5). The discrepancies arose from oxidation-rate variations under full-oxidation assumptions that alter pathway quantification.

Quantitative pathway apportionment of sulfate formation was achieved through systematic evaluation of reaction-specific α values derived for each SO_2 oxidation mechanism. The results demonstrate that TMI-catalyzed and NO_2-mediated oxidation pathways collectively dominate atmospheric sulfate production across all considered oxidation scenarios. Notably, complete-oxidation assumptions systematically underestimate the TMI pathway contribution compared to partial-oxidation models, as revealed by isotopic mass balance calculations. This systematic bias originates from neglecting kinetic fractionation effects during intermediate oxidation stages, particularly under high aerosol acidity conditions where TMI chemistry prevails. The persistent dominance of these two pathways persists despite varying meteorological conditions and emission profiles, suggesting their fundamental role in sulfur cycling.

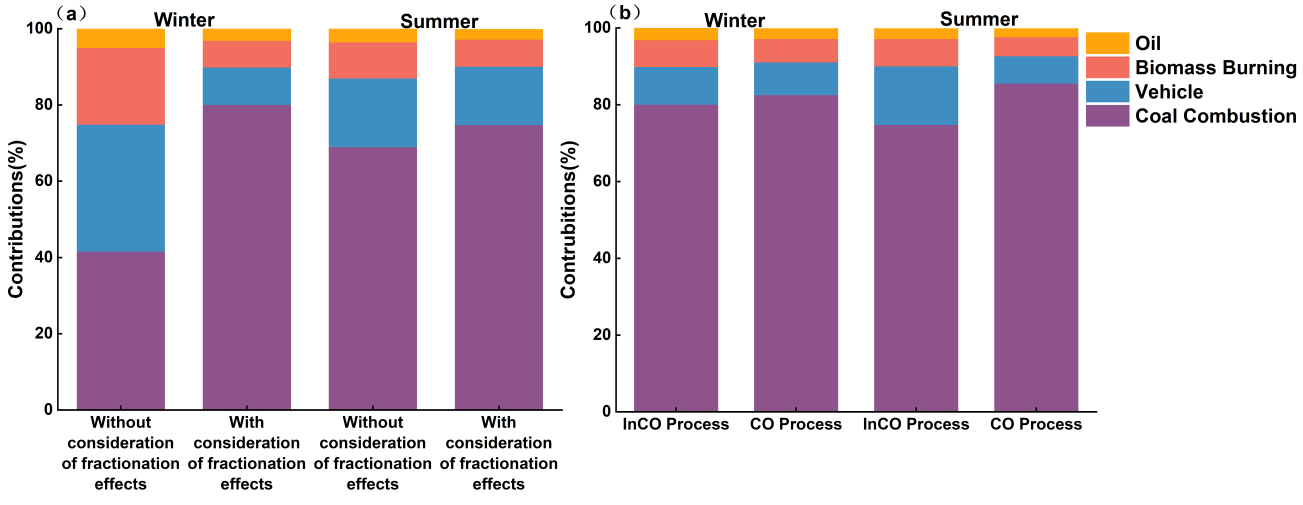

Figure 6. (a) Seasonal variations of source apportionments to sulfate aerosols in Nanjing. (b) Source apportionments of sulfate aerosols in Nanjing resolved by the SIAR model with consideration of fractionation effects under InCO Process and CO Process.

Quantitative source apportionment of atmospheric sulfate was achieved through coupled $\delta^{34}S-SO_4^{2-}$ measurements and Bayesian isotopic mixing models, requiring emission source-specific $\delta^{34}S$ signatures as critical input parameters. Correction for sulfur isotopic fractionation during $SO_2-to-SO_4^{2-}$ conversion is essential, as this process enriches $\delta^{34}S$ values by 1.2–7.2‰(Lin et al., 2022), necessitating subtraction of pathway-specific fractionation coefficients prior to source quantification. Neglecting fractionation effects distorts source contributions, yielding winter estimates of 41.5% (coal), 5.2% (oil), 20.1% (biomass), and 33.3% (vehicle), alongside summer values of 68.9%, 3.6%, 9.5%, and 18.0% (Fig.6a) respectively-results that inaccurately emphasize traffic emissions contrary to regional emission inventories and chemical transport modeling. Incorporating fractionation factors resolves this discrepancy, aligning sulfate sources with inventory data where coal combustion dominates annually, while idealized complete-oxidation models underestimate summer vehicle contributions by 8.2% and

https://doi.org/10.5194/egusphere-2025-6533
Preprint. Discussion started: 12 February 2026

overestimate coal combustion proportions (about 10.8%) by comparable margins despite minimal winter deviations. This systematic validation underscores the requirement for fractionation correction in isotope-based atmospheric sulfate sourcing.

4 Conclusions

This study establishes a paradigm shift in atmospheric sulfate source apportionment by advancing beyond conventional isotopic models constrained by idealized SO_2 oxidation assumptions. Through the integration of field-observed oxidation kinetics with optimized isotopic fractionation corrections, we demonstrate the predominance of TMI-catalyzed and NO_2-mediated pathways in sulfate formation, with coal combustion (summer overestimation: 10.8%) and traffic emissions (summer underestimation: 8.2%) (Fig.6b) identified as dominant sources. Crucially, comparative model analysis reveals systematic biases in traditional complete-oxidation frameworks, which disproportionately diminish TMI pathway contributions while misallocating source-specific burdens. These methodological refinements enhancing the precision of stable isotope tracing techniques relative error margin, and reconciling long-standing discrepancies between isotopic, inventory-based, and transport-modeling approaches in particulate matter source attribution. The validated framework provides actionable scientific basis for targeted emission control strategies, particularly in addressing combustion-related sulfate precursors across seasonal variations.

Code availability. Data used in this study are available upon request to the corresponding author.

Data availability. The data underlying the findings of this study are available from the corresponding author upon reasonable request.

Code and data availability. Global data assimilation system (GDAS) data were obtained from the multi-scale meteorological dataset pro vided by the National Centers for Environmental Prediction in the United States (http://www.ready.noaa.gov/hypub-bin/trajtype.pl). The stable isotope mixing models in R is an upgraded version of the SIAR package, and it has many similar functionalities. This new version includes more complex mixing models and has advanced plotting capabilities (http://cran.r-project.org/web/packages/simmr/vignettes/simmr.html).

Author contributions. Z.-B.G. designed the research. X.-X.B. performed the model experiments. J G. analyzed the data. Z.-Z.X. and Q.-W.A.:conceptualization, methodology, software, investigation, funding acquisition, resources, data curation, validation, formal analysis. Q.-J.G. and S.-S.M. methodology, investigation, and software. X.-X.B. and P.-X.Q. prepared the manuscript and all co-authors helped improve the manuscript.

https://doi.org/10.5194/egusphere-2025-6533
Preprint. Discussion started: 12 February 2026

Competing interests. The authors declare no competing financial interest.

Acknowledgements. This work was supported by the National Natural Science Foundation of China (42473024).

https://doi.org/10.5194/egusphere-2025-6533
Preprint. Discussion started: 12 February 2026

References

Arimoto, R., Duce, R., Savoie, D., Prospero, J., Talbot, R., Cullen, J., Tomza, U., Lewis, N., and Ray, B.: Relationships among aerosol constituents from Asia and the North Pacific during PEM-West A, Journal of Geophysical Research: Atmospheres, 101, 2011–2023, https://doi.org/10.1029/95JD01071, 1996.

Fan, M.-Y., Zhang, Y.-L., Lin, Y.-C., Cao, F., Zhao, Z.-Y., Sun, Y., Qiu, Y., Fu, P., and Wang, Y.: Changes of emission sources to nitrate aerosols in Beijing after the clean air actions: Evidence from dual isotope compositions, Journal of Geophysical Research: Atmospheres, 125, e2019JD031 998, https://doi.org/10.1029/2019JD031998, 2020a.

Fan, M.-Y., Zhang, Y.-L., Lin, Y.-C., Li, J., Cheng, H., An, N., Sun, Y., Qiu, Y., Cao, F., and Fu, P.: Roles of sulfur oxidation pathways in the variability in stable sulfur isotopic composition of sulfate aerosols at an urban site in Beijing, China, Environmental Science & Technology Letters, 7, 883–888, https://doi.org/10.1021/acs.estlett.0c00623, 2020b.

Fan, M.-Y., Zhang, Y.-L., Lin, Y.-C., Li, J., Cheng, H., An, N., Sun, Y., Qiu, Y., Cao, F., and Fu, P.: Roles of sulfur oxidation pathways in the variability in stable sulfur isotopic composition of sulfate aerosols at an urban site in Beijing, China, Environmental Science & Technology Letters, 7, 883–888, https://doi.org/10.1021/acs.estlett.0c00623, 2020c.

Guo, Z., Guo, Q., Chen, S., Zhu, B., Zhang, Y., Yu, J., and Guo, Z.: Study on pollution behavior and sulfate formation during the typical haze event in Nanjing with water soluble inorganic ions and sulfur isotopes, Atmospheric Research, 217, 198–207, https://doi.org/10.1016/j.atmosres.2018.11.009, 2019.

Han, X., Guo, Q., Liu, C., Fu, P., Strauss, H., Yang, J., Hu, J., Wei, L., Ren, H., Peters, M., et al.: Using stable isotopes to trace sources and formation processes of sulfate aerosols from Beijing, China, Scientific Reports, 6, 29 958, https://doi.org/10.1038/srep29958, 2016.

Han, X., Lang, Y., Guo, Q., Li, X., Ding, H., and Li, S.: Enhanced oxidation of SO_2 by H_2O_2 during haze events: Constraints from sulfur isotopes, Journal of Geophysical Research: Atmospheres, 127, e2022JD036 960, https://doi.org/10.1073/pnas.2408199121, 2022.

Harris, E., Sinha, B., Hoppe, P., Crowley, J., Ono, S., and Foley, S.: Sulfur isotope fractionation during oxidation of sulfur dioxide: gas-phase oxidation by OH radicals and aqueous oxidation by H_2O_2, O_3 and iron catalysis, Atmospheric Chemistry and Physics, 12, 407–423, https://doi.org/10.1109/50.983245, 2012a.

Harris, E., Sinha, B., Hoppe, P., Foley, S., and Borrmann, S.: Fractionation of sulfur isotopes during heterogeneous oxidation of SO 2 on sea salt aerosol: a new tool to investigate non-sea salt sulfate production in the marine boundary layer, Atmospheric Chemistry and Physics, 12, 4619–4631, https://doi.org/10.5194/acp-12-4619-2012, 2012b.

Kang, Y., Liu, M., Song, Y., Huang, X., Yao, H., Cai, X., Zhang, H., Kang, L., Liu, X., Yan, X., He, H., Zhang, Q., Shao, M., and Zhu, T.: High-resolution ammonia emissions inventories in China from 1980 to 2012, Atmospheric Chemistry and Physics, 16, 2043–2058, https://doi.org/10.5194/acp-16-2043-2016, 2016.

Li, J., Zhang, Y.-L., Cao, F., Zhang, W., Fan, M., Lee, X., and Michalski, G.: Stable sulfur isotopes revealed a major role of transition-metal ion-catalyzed SO_2 oxidation in haze episodes, Environmental Science & Technology, 54, 2626–2634, https://doi.org/10.1021/acs.est.9b07150, 2020.

Lin, Y.-C., Yu, M., Xie, F., and Zhang, Y.: Anthropogenic emission sources of sulfate aerosols in Hangzhou, East China: Insights from isotope techniques with consideration of fractionation effects between gas-to-particle transformations, Environmental Science & Technology, 56, 3905–3914, https://doi.org/10.1021/acs.est.1c05823, 2022.

https://doi.org/10.5194/egusphere-2025-6533
Preprint. Discussion started: 12 February 2026

Mang, L., Xiaolin, Z., Menghan, L., Yilun, X., Zhisheng, Z., Jun, T., Binbin, S., Lanzhong, L., Yanan, S., and Thiemens, M. H.: Five-S-isotope evidence of two distinct mass-independent sulfur isotope effects and implications for the modern and Archean atmospheres, Proceedings of the National Academy of Sciences, pp. 201803 420–, https://doi.org/10.1073/pnas.1803420115, 2018.

Novák, M., Jacˇková, I., and Přechová, E.: Temporal trends in the isotope signature of air-borne sulfur in Central Europe, Environmental science & technology, 35, 255–260, https://doi.org/10.1021/es0000753, 2001.

Parnell, A. C., Inger, R., Bearhop, S., and Jackson, A. L.: Source partitioning using stable isotopes: coping with too much variation, PloS one, 5, e9672, https://doi.org/10.1371/journal.pone.0009672, 2010.

Sinha, B.: High-Precision Measurements of ^{33}S and ^{34}S Fractionation during SO_2 Oxidation Reveal Causes of Seasonality in SO_2 and Sulfate Isotopic Composition, https://doi.org/10.1021/es402824c, 2013.

Tao, J., Gao, J., Zhang, L., Zhang, R., Che, H., Zhang, Z., Lin, Z., Jing, J., Cao, J., and Hsu, S.-C.: $PM_{2.5}$ pollution in a megacity of southwest China: source apportionment and implication, Atmospheric Chemistry and Physics, 14, 8679–8699, https://doi.org/10.5194/acp-14-8679-2014, 2014a.

Tao, J., Zhang, L., Ho, K., Zhang, R., Lin, Z., Zhang, Z., Lin, M., Cao, J., Liu, S., and Wang, G.: Impact of $PM_{2.5}$ chemical compositions on aerosol light scattering in Guangzhou—the largest megacity in South China, Atmospheric Research, 135, 48–58, https://doi.org/10.1016/j.atmosres.2013.08.015, 2014b.

Wei, L., Yue, S., Zhao, W., Yang, W., Zhang, Y., Ren, L., Han, X., Guo, Q., Sun, Y., Wang, Z., et al.: Stable sulfur isotope ratios and chemical compositions of fine aerosols ($PM_{2.5}$) in Beijing, China, Science of the Total Environment, 633, 1156–1164, https://doi.org/10.1016/j.scitotenv.2018.03.153, 2018.

Xiao, H.-W., Xiao, H.-Y., Long, A.-M., Wang, Y.-L., and Liu, C.-Q.: Sources and meteorological factors that control seasonal variation of $\delta^{34}S$ values in rainwater, Atmospheric research, 149, 154–165, https://doi.org/10.1016/j.atmosres.2014.06.003, 2014.

Yang, R., Lou, Q., Wang, M., Cao, L., and Luo, L.: Using Stable Sulfur Isotopes to Quantify the Formation Mechanism and Sources of SO_4^{2-} in $PM_{2.5}$ in Haikou City, ACS Earth and Space Chemistry, 9, 560–568, https://doi.org/10.1021/acsearthspacechem.4c00304, 2025.

Yao, X., Chan, C. K., Fang, M., Cadle, S., Chan, T., Mulawa, P., He, K., and Ye, B.: The water-soluble ionic composition of $PM_{2.5}$ in Shanghai and Beijing, China, Atmospheric Environment, 36, 4223–4234, https://doi.org/10.1016/S1352-2310(02)00342-4, 2002.

Zheng, M., Song, D., Zhang, D., Cao, Y., and Fan, H.: Using sulfur isotopes to constrain the sources of sulfate in $PM_{2.5}$ during the winter in Jiaozuo City, Atmospheric Environment, 332, 120 618, https://doi.org/10.1016/j.atmosenv.2024.120618, 2024.